Supporting Information

Magnetocaloric Effect of Two Gd−based Frameworks

Bo−Liang Liu, Qiao−Fei Xu, La−Sheng Long,* and Lan−Sun Zheng

Collaborative Innovation Center of Chemistry for Energy Materials, State Key Laboratory of Physical Chemistry of Solid Surfaces and Department of Chemistry, College of Chemistry and Chemical Engineering, Xiamen University, Xiamen, 361005, China.

Experimental Section

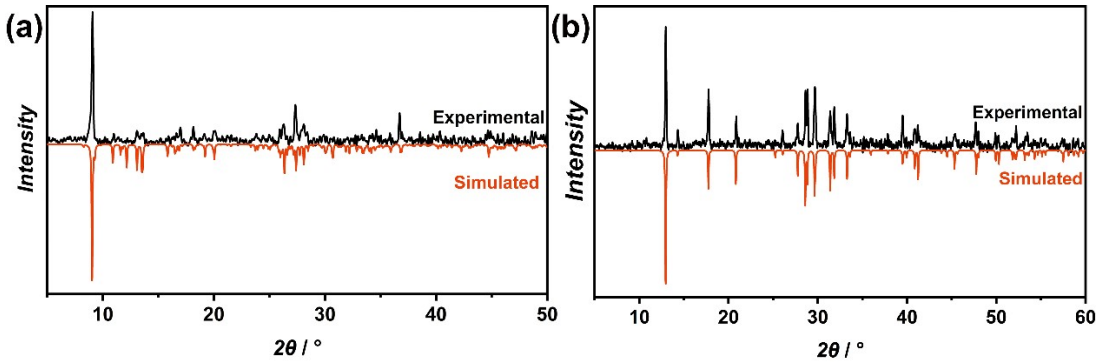

Figure S1. PXRD patterns for **1** (a) and **2** (b).

The PXRD patterns are consistent with the simulated ones based on the single−crystal structure determinations, suggesting the phase purity of **1** and **2**.

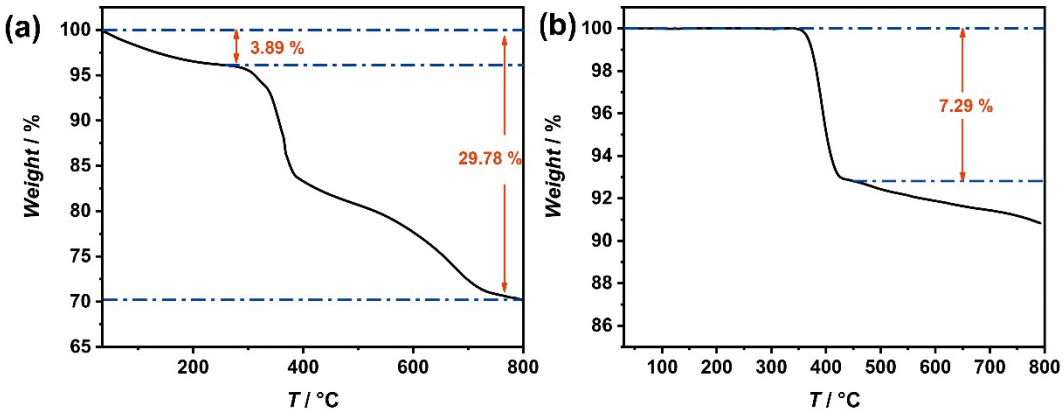

Figure S2. TGA curve of **1** (a) and **2** (b).

The TGA curve of **1** and **2** was carried out under N_2 atmosphere. With temperature rising, **1** lost weight sustainedly, while **2** remained stable up to 350 °C. By the end of 265 ºC, the weight loss of **1** is up to 3.89 %, attributed to the loss of 2.5 H_2O. The final weight loss is up to 29.78 %, which matches the theoretical value 30.31 % calculated for Gd_2O_3 as the residue. For **2**, when the temperature was raised to 430 °C, the weight loss of 7.29% matches well with that of 7.52% calculated by two H_2O indicating that the residue is $Gd_2O_2SO_4$ at 430 ºC. As the temperature rising up, the decrease of the curve attributes to the decomposition of SO_4^{2-}. Due to the limitations of the instrument, the following process will not be discussed.

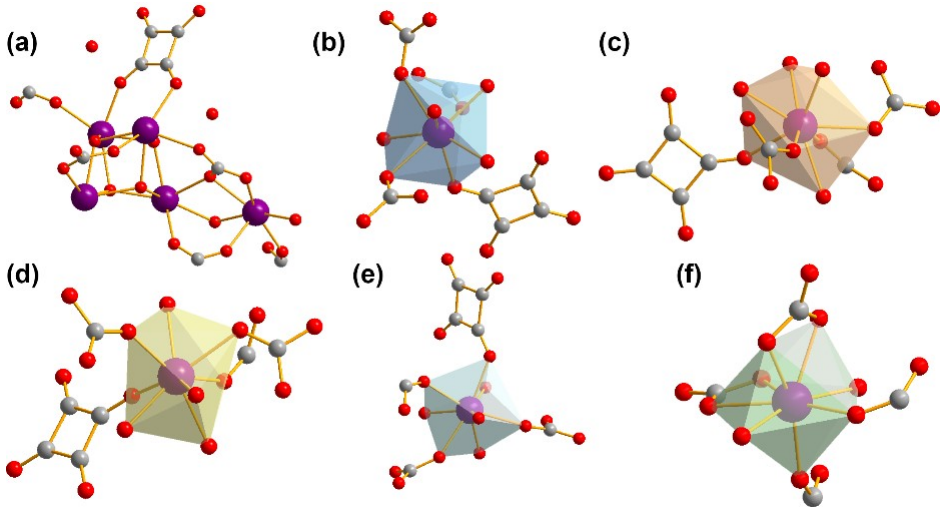

Figure S3. (a) Asymmetric unit of **1**; Coordination environment of Gd^{3+} in **1**: Gd1 (b), Gd2 (c), Gd3 (d), Gd4 (e), Gd5 (f). (Purple: Gd; Red: O; Grey: C)

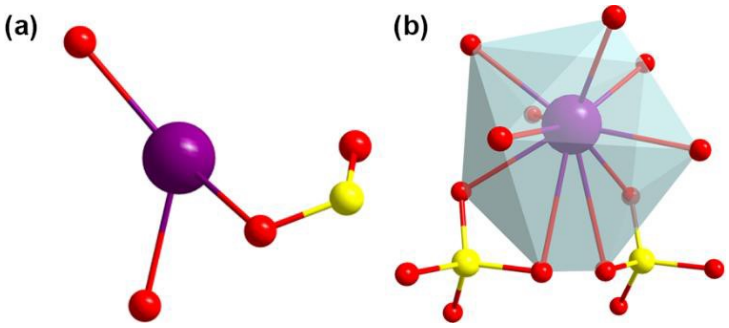

Figure S4. (a) Asymmetric unit of **2**; (b) Coordination environment of Gd^{3+} in **2**. (Purple: Gd; Red: O; Yellow: S)

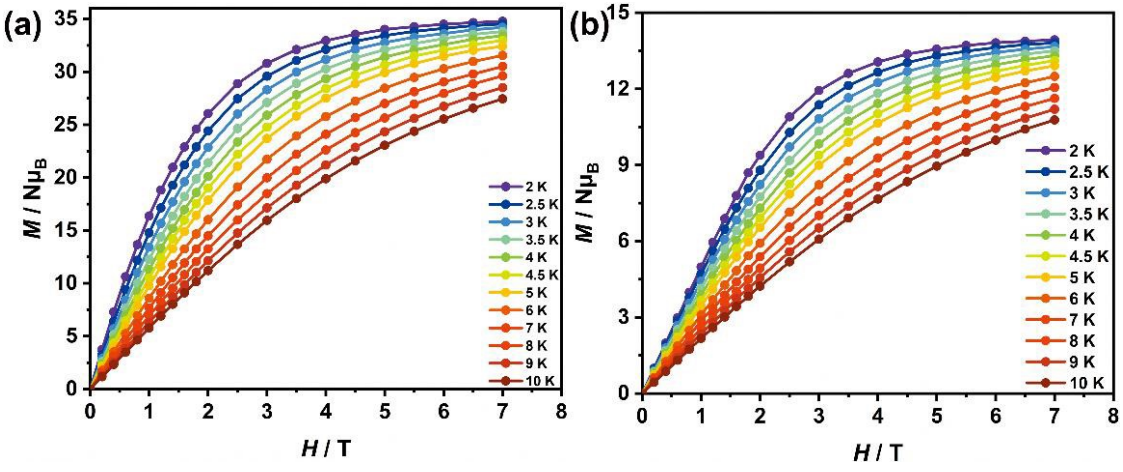

Figure S5. Plot of field−dependent magnetizations at 2−10 K for **1** (a) and **2** (b).

Table S1. BVS [1] calculations for oxygen atoms in the main structure of **1**.

Atom	Bond	R_{ij}	R_0	S_{ij}	Assignment
O1	Gd–O	2.436	2.031	0.335	**OH⁻**
	Gd–O	2.400		0.369	
	Gd–O	2.353		0.419	
	Total			**1.123**	
O2	Gd–O	2.438	2.031	0.333	**OH⁻**
	Gd–O	2.412		0.357	
	Gd–O	2.398		0.371	
	Total			**1.061**	
O4	Gd–O	2.399	2.031	0.370	**OH⁻**
	Gd–O	2.372		0.398	
	Gd–O	2.358		0.413	
	Total			**1.181**	
O6	Gd–O	2.426	2.031	0.344	**OH⁻**
	Gd–O	2.411		0.358	
	Gd–O	2.372		0.398	
	Total			**1.100**	
O7	Gd–O	2.422	2.031	0.348	**OH⁻**
	Gd–O	2.422		0.348	
	Gd–O	2.416		0.353	
	Total			**1.048**	
O17	Gd–O	2.406	2.031	0.363	**OH⁻**
	Gd–O	2.384		0.385	
	Gd–O	2.383		0.386	
	Total			**1.134**	

Table S2. BVS calculations for oxygen atoms in **2**.

Atom	Bond	R_{ij}	R_0	S_{ij}	Assignment
O1	Gd–O	2.439	2.031	0.332	**OH⁻**
	Gd–O	2.439		0.332	
	Gd–O	2.399		0.370	
	Total			**1.034**	
O2	Gd–O	2.385	2.031	0.384	**OH⁻**
	Gd–O	2.375		0.395	
	Gd–O	2.375		0.395	
	Total			**1.174**	

The bond valence sum (BVS) analysis was used to determine the oxidation states of oxygen atoms in compound **1** and **2**. The calculation formula is $S_{ij} = \exp[(R_0–R_{ij})/b]$, in which S_{ij} is the valence of the individual bond, R_{ij} is the observed bond length, R_0 is a constant depended upon the bonded elements, and b is a constant of 0.37. As shown in Table S1 and Table S2, the total BVS values of O atoms are very close to the state of +1, for which we identify the states of all O atoms are assigned to hydroxyl groups.

Table S3. Crystal data for **1** and **2**.

Compound	**1**	**2**
Formula	$C_9H_{12}Gd_5O_{24.5}$	$Gd_2H_4O_8S$
Formula weight	1300.45	478.59
Temperature/K	294	100
Crystal system	Monoclinic	Monoclinic
Space group	$P2_1/c$	$C2/m$
a / Å	10.909 (2)	13.832 (3)
b / Å	10.909 (2)	3.650 (6)
c / Å	20.068 (3)	6.268 (13)
α / º	90	90
β / º	101.748 (2)	99.07 (2)
γ / º	90	90
V / Å^3	2342.02 (15)	312.45 (11)
Z	4	2
D_c / g cm^{-3}	3.688	5.087
μ / mm^{-1}	91.08	139.16
θ / º	4.1−75.2	6.5−72.2
Observed reflections	13543	1257
F(000)	2336	424
GOOF	1.060	1.117
$R_1[I > 2\sigma(I)]$[a]	0.029	0.066
wR_2(All data)[b]	0.071	0.164

[a] $R_1 = \sum ||Fo| - |Fc|| / \sum |Fo|$ [b] $wR_2 = \{\sum[w(Fo^2 - Fc^2)^2] / \sum[w(Fo^2)^2]\}^{1/2}$

Table S4. The Continuous Shape Measurements (CShM) [2] of **1**.

	Gd				
	Gd1	Gd2	Gd3	Gd4	Gd5
OP−8 (D_{8h})	31.143	30.200	30.513	30.857	31.702
HPY−8 (C_{7v})	23.254	23.178	22.288	22.625	22.206
HBPY−8 (D_{6h})	14.389	14.825	15.391	15.972	16.370
CU−8 (O_h)	7.986	8.494	9.450	9.914	14.878
SAPR−8 (D_{4d})	2.761	2.369	**0.998**	**1.162**	6.828
TDD−8 (D_{2d})	**0.249**	**0.275**	1.620	1.358	4.786
JGBF−8 (D_{2d})	14.802	14.523	15.750	14.956	14.217
JETBPY−8 (D_{3h})	28.673	28.951	28.533	28.784	25.037
JBTP−8 (C_{2v})	3.126	2.895	2.392	2.242	5.025
BTPR−8 (C_{2v})	2.593	2.412	1.546	1.483	**4.142**
JSD−8 (D_{2d})	3.002	2.829	4.629	4.060	6.501
TT−8 (T_d)	8.849	9.335	10.074	10.585	15.611
ETBPY−8 (D_{3h})	24.758	24.628	23.570	24.051	21.351

OP−8 = Octagon, D_{8h}; HPY−8 = Heptagonal pyramid, C_{7v}; HBPY−8 = Hexagonal bipyramid, D_{6h}; CU−8 = Cube, O_h; SAPR−8 = Square antiprism, D_{4d}; TDD−8 = Triangular dodecahedron, D_{2d}; JGBF−8 = Johnson−Gyrobifastigium J26, D_{2d}; JETBPY−8 = Johnson−Elongated triangular bipyramid J14, D_{3h}; JBTP−8 = Johnson−Biaugmented trigonal prism J50, C_{2v}; BTPR−8 = Biaugmented trigonal prism, C_{2v}; JSD−8= Snub disphenoid J84, D_{2d}; TT−8= Triakis tetrahedron, T_d; ETBPY−8 =Elongated trigonal bipyramid, D_{3h}.

Table S5. The Continuous Shape Measurements (CShM) of **2**.

	Gd
DP−10 (D_{8h})	32.174
EPY−10 (C_{9v})	18.989
OBPY−10 (D_{8h})	19.270
PPR−10 (D_{5h})	14.624
PAPR−10 (D_{5d})	14.707
JBCCU−10 (D_{4h})	18.264
JBCSAPR−10 (D_{4d})	12.582
JMBIC−10 (C_{2v})	**5.163**
JATDI−10 (C_{3v})	16.184
JSPC−10 (C_{2v})	9.240
SDD−10 (D_2)	9.397
TD−10 (C_{2v})	9.325
HD−10 (D_{4h})	15.205

DP−10 = Decagon; EPY−10 = Enneagonal pyramid; OBPY−10 = Octagonal bipyramid; PPR−10 = Pentagonal prism; PAPR−10 = Pentagonal antiprism; JBCCU−10 = Bicapped cube; JBCSAPR−10 = Bicapped square antiprism; JMBIC−10 = Metabidiminished icosahedron; JATDI−10 = Augmented tridiminished icosahedron; JSPC−10 = Sphenocorona; SDD−10 = Staggered Dodecahedron; TD−10 = Tetradecahedron; HD−10 = Hexadecahedron.

Table S6. Selected bond distances (Å) and bond angles (°) of **1**.

Gd1—O1	2.436 (4)	O1—Gd2i	2.400 (4)
Gd1—O4i	2.399 (4)	O2—Gd4iv	2.412 (4)
Gd1—O5	2.412 (4)	O3—Gd4viii	2.400 (4)
Gd1—O6	2.426 (4)	O3—Gd5iii	2.438 (4)
Gd1—O12	2.312 (5)	O4—Gd1iv	2.399 (4)
Gd1—O17	2.383 (4)	O6—Gd2iii	2.411 (4)
Gd1—O18ii	2.443 (4)	O7—Gd3v	2.416 (4)
Gd1—O21iii	2.400 (5)	O7—Gd4ix	2.422 (4)
Gd2—O1iv	2.400 (4)	O8—Gd5iii	2.435 (5)
Gd2—O2	2.438 (4)	O9—Gd4ix	2.425 (5)
Gd2—O4	2.358 (4)	O10—Gd3v	2.425 (4)
Gd2—O6iii	2.411 (4)	O14—Gd3x	2.505 (4)
Gd2—O8	2.392 (5)	O14—Gd4iv	2.516 (5)
Gd2—O13	2.307 (5)	O17—Gd3i	2.406 (4)
Gd2—O15	2.425 (5)	O18—Gd1xi	2.443 (4)
Gd2—O18iv	2.459 (4)	O18—Gd2i	2.459 (4)
Gd3—O2	2.398 (4)	O19—Gd3v	2.426 (5)
Gd3—O4	2.372 (4)	O21—Gd1iii	2.400 (5)
Gd3—O7v	2.416 (4)	Gd4—O14i	2.516 (5)
Gd3—O10v	2.425 (4)	Gd4—O17	2.384 (4)
Gd3—O11	2.418 (5)	Gd4—O22	2.445 (5)
Gd3—O14vi	2.505 (4)	Gd5—O3iii	2.438 (4)
Gd3—O17iv	2.406 (4)	Gd5—O5	2.432 (5)
Gd3—O19v	2.426 (5)	Gd5—O6	2.372 (4)
Gd4—O1	2.353 (4)	Gd5—O7	2.422 (4)
Gd4—O2i	2.412 (4)	Gd5—O8iii	2.435 (5)
Gd4—O3viii	2.400 (4)	Gd5—O10	2.432 (4)
Gd4—O7vii	2.422 (4)	Gd5—O16	2.320 (5)

Gd4—O9vii	2.425 (5)	Gd5—O20	2.298 (6)
Gd2i—O1—Gd1	104.37 (14)	Gd5—O6—Gd1	111.93 (16)
Gd4—O1—Gd1	106.04 (15)	Gd5—O6—Gd2iii	110.32 (16)
Gd4—O1—Gd2i	108.67 (16)	Gd3v—O7—Gd4ix	116.37 (16)
Gd3—O2—Gd2	104.74 (15)	Gd3v—O7—Gd5	109.34 (16)
Gd3—O2—Gd4iv	107.38 (15)	Gd5—O7—Gd4ix	107.25 (15)
Gd4iv—O2—Gd2	105.54 (15)	Gd2—O8—Gd5iii	108.81 (17)
Gd4viii—O3—Gd5iii	107.46 (17)	Gd3v—O10—Gd5	108.68 (16)
Gd2—O4—Gd1iv	106.86 (15)	Gd3x—O14—Gd4iv	109.93 (17)
Gd2—O4—Gd3	108.14 (16)	Gd1—O17—Gd3i	105.60 (15)
Gd3—O4—Gd1iv	106.20 (15)	Gd1—O17—Gd4	106.75 (16)
Gd1—O5—Gd5	110.33 (17)	Gd4—O17—Gd3i	108.02 (16)
Gd2iii—O6—Gd1	110.86 (16)	Gd1xi—O18—Gd2i	108.69 (16)

Symmetry codes: (i) x, $-y+1/2$, $z+1/2$; (ii) $-x+1$, $y+1/2$, $-z+3/2$; (iii) $-x+1$, $-y+1$, $-z+1$; (iv) x, $-y+1/2$, $z-1/2$; (v) $-x+1$, $-y$, $-z+1$; (vi) $-x$, $y-1/2$, $-z+1/2$; (vii) $x-1$, y, z; (viii) $-x$, $-y+1$, $-z+1$; (ix) $x+1$, y, z; (x) $-x$, $y+1/2$, $-z+1/2$; (xi) $-x+1$, $y-1/2$, $-z+3/2$.

Table S7. Selected bond distances (Å) and bond angles (°) of **2**.

Gd1—O3ii	2.518 (10)	Gd1—O1v	2.439 (9)
Gd1—O3	2.518 (10)	Gd1—O1	2.399 (15)
Gd1—O2iii	2.375 (8)	Gd1—O1vi	2.439 (9)
Gd1—O2iv	2.375 (8)	Gd1—O2	2.385 (13)
Gd1i—O3—Gd1	92.9 (5)	Gd1—O1—Gd1vi	109.0 (4)
Gd1iii—O2—Gd1	110.8 (4)	Gd1vi—O1—Gd1v	96.8 (5)
Gd1iv—O2—Gd1iii	100.4 (5)	Gd1—O1—Gd1v	109.0 (4)
Gd1iv—O2—Gd1	110.8 (4)		

Symmetry codes: (i) x, $y-1$, z; (ii) x, $y+1$, z; (iii) $-x+3/2$, $-y+3/2$, $-z+1$; (iv) $-x+3/2$, $-y+5/2$, $-z+1$; (v) $-x+3/2$, $-y+3/2$, $-z+2$; (vi) $-x+3/2$, $-y+5/2$, $-z+2$.

Reference

(1) Brown, I. D.; Altermatt, D. Bond-Valence Parameters Obtained from a Systematic Analysis of the Inorganic Crystal Structure Database. *Acta Cryst. B* **1985**, *41*, 244–247.

(2) Alvarez, S.; Alemany, P.; Casanova, D.; Cirera, J.; Llunell, M.; Avnir, D. Shape Maps and Polyhedral Interconversion Paths in Transition Metal Chemistry. *Coord. Chem. Rev.* **2005**, *249*, 1693–1708.